A Multi-Grid Method for Transonic Wing Analysis and Design

Pradeep Raj*
Lockheed-California Company, Burbank, California

A fixed full-multigrid, full-approximation scheme has been incorporated into the solution algorithm of the full-potential finite-difference code FLO-22, widely used for analyzing wings of arbitrary planforms in transonic flows. The computational efficiency of the code is significantly enhanced by this modification. More accurate simulation of flow fields, especially for tapered wings, results from the use of planform conforming mesh. In addition to improved analysis capability, the new code, labeled FLO-22.5, contains a design option. All or some of the sections of a wing are computationally recontoured to achieve a desired pressure distribution. The surface modification is dictated by the difference between the distributions obtained by analyzing the baseline geometry and the specified target pressure levels.

Nomenclature

A,B,C = coefficients in transformed full-potential equation, Eq. (2)
C_L = lift coefficient
C_p = pressure coefficient
c = local chord
D = coefficient in Eq. (2)
D^k = sequence of grids
E,F = coefficient in Eq. (2)
F^k = forcing term in Eq. (3)
F_1,F_2 = scale factors in parabolic transformation
G = reduced potential
h = mesh spacing
L = difference operator in Eq. (3)
M = freestream Mach number
m = total number of meshes
n = order of meshes in multigrid scheme ($n=1$, coarsest)
P = prolongation operator
R = forcing term in transformed FPE, Eq. (2); also restriction operator
X,Y,Z = sheared parabolic coordinates
x,y,z = Cartesian coordinates; x = chordwise, z = spanwise
x_s,y_s = singular point coordinates
α = angle of attack
Γ = circulation at root station
τ = truncation error
Φ = velocity potential

Subscripts

X,Y,Z = partial derivatives
k = grid level in multigrid scheme

Superscript

k = grid level in multigrid scheme

Introduction

A NUMBER of computational methods are currently available for three-dimensional transonic flow simulation. These methods vary in complexity of mathematical models used and in their capability to model complex geometries. At one end of the spectrum are methods[1,2] based on the transonic small perturbation equation. They are capable of analyzing flows about complete aircraft configurations. This is facilitated by the application of boundary conditions on mean surfaces. At the other end are methods based on Reynolds averaged Navier-Stokes equations[3] and Euler equations[4] which are not yet mature enough for routine applications. The gap between these approaches is presently bridged by the full-potential equation (FPE). Several computer codes based on this formulation have been developed over the past decade for analyzing isolated wings[5-8] and wing-fuselage combinations.[9,10] For routine practical applications, the FLO-22 code,[5] using a nonconservative finite-difference approximation to the FPE, is widely used in the aircraft industry. Its use is strongly supported by extensive correlation of computational results with experimental data.[11-14]

The widespread use of the FLO-22 code has also prompted a variety of modifications to overcome some of its limitations. Among these, the wing-alone restriction is partially alleviated by replacing the zero normal velocity on the plane of symmetry by a prescribed nonzero normal velocity. The latter may be approximated to varying degrees of accuracy, e.g., a perturbation velocity due to fuselage alone using linearized analytical formulation[12] or the velocity field obtained from a linear, subsonic, panel method.[14]

The inviscid formulation places additional restrictions on accurate flow simulation, especially about aft-loaded supercritical wings. For these wings it is important to compute the surface pressure distribution that reflects the effect of boundary layer on the surface geometry. This may be accomplished through interactive potential-flow/boundary-layer computations.[13,14] The inaccuracies in predicting the value of drag force by the classical approach of integrating the streamwise component of computed pressure around the wing have been reduced considerably, as described in Refs. 13 and 14. In addition, methods for designing wings have been developed[15,16] that employ the FLO-22 code as the basic tool. Consequently, modified versions of this code are very useful for analyzing and designing advanced technology supercritical wings.

This paper addresses two aspects of the code that can be improved to further enhance its effectiveness. The first one involves geometric transformations to produce computational grids. In the existing versions, the grid has fewer points on the outboard stations than on the inboard ones for tapered wings. This feature limits the accuracy of flow simulation. Results in this paper illustrate the problem and validate the proposed

Received May 16, 1983; revision received Oct. 25, 1983.

*Senior Research Specialist, Computational Aerodynamics Department. Member AIAA.

means of correcting it. The second aspect concerns the computational efficiency of the code. The difference equations are presently solved by the successive line over relaxation (SLOR) algorithm. Such an algorithm is local by nature, i.e., each grid point is influenced solely by information from adjacent points. Consequently, the global transmission of information slows asymptotically with distance. The rate of convergence deteriorates further with increasing density of the mesh. To remedy this difficulty, the use of a multigrid technique has been advocated by Brandt.[17] Its effectiveness for elliptic problems has been well documented in Ref. 18. Extension of this technique to the three-dimensional mixed hyperbolic-elliptic problems of transonic flows has been demonstrated by McCarthy and Reyhner[19] and Shmilovich and Caughey.[20]

In the following sections, incorporation of 1) a modified transformation to produce planform conforming grid, and 2) a multigrid solution algorithm into the FLO-22 code, is described. The resulting code, labeled FLO-22.5, exhibits significant improvements in accuracy and computational efficiency as demonstrated by the results presented here.

Planform Conforming Grid

The FLO-22 code solves a finite difference approximation to the full-potential equation in a sheared parabolic coordinate system. The mapping from the physical space (x,y,z) to the computational space (X,Y,Z) is given by:

$$x = F_1 (X^2 - Y^2)/2 + x_s(z)$$
$$y = F_1 XY + y_s(z) \qquad (1)$$
$$z = F_2 Z$$

where F_1 and F_2 are scale factors and $x_s(z), y_s(z)$ define a singular line. In the transformed domain, the FPE is rewritten as:

$$AG_{XX} + BG_{YY} + CG_{ZZ} + DG_{XY} + EG_{XZ} + FG_{YZ} + R = 0 \qquad (2)$$

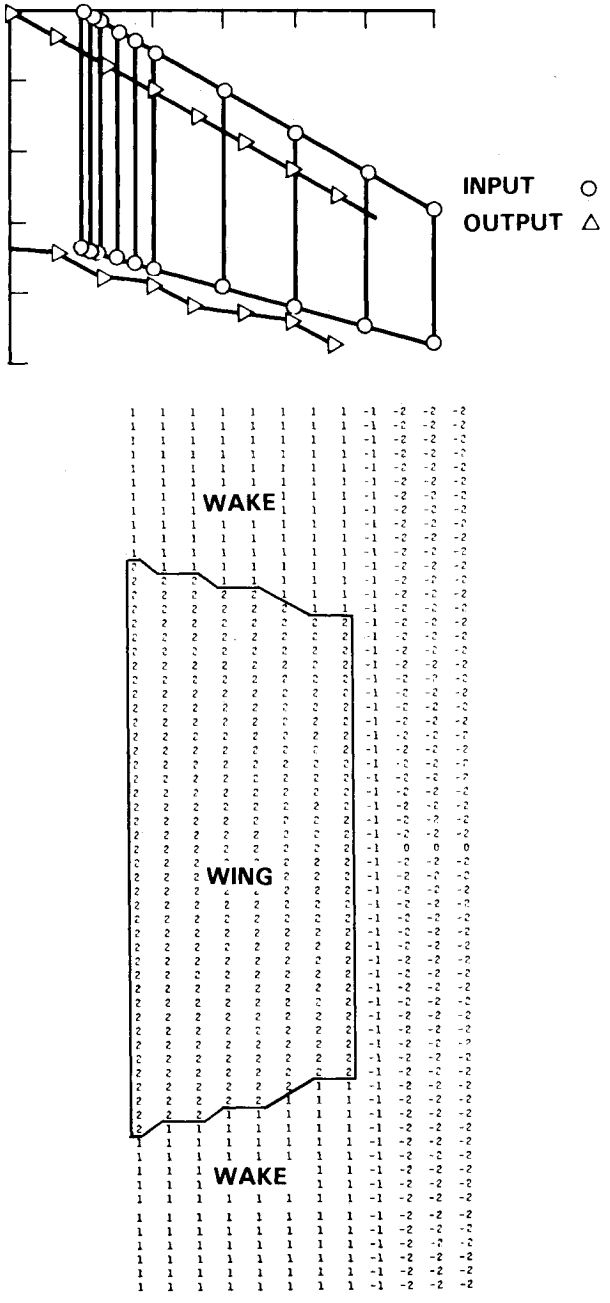

Fig. 1a Wing planform in physical and mapped computational planes in FLO-22 code.

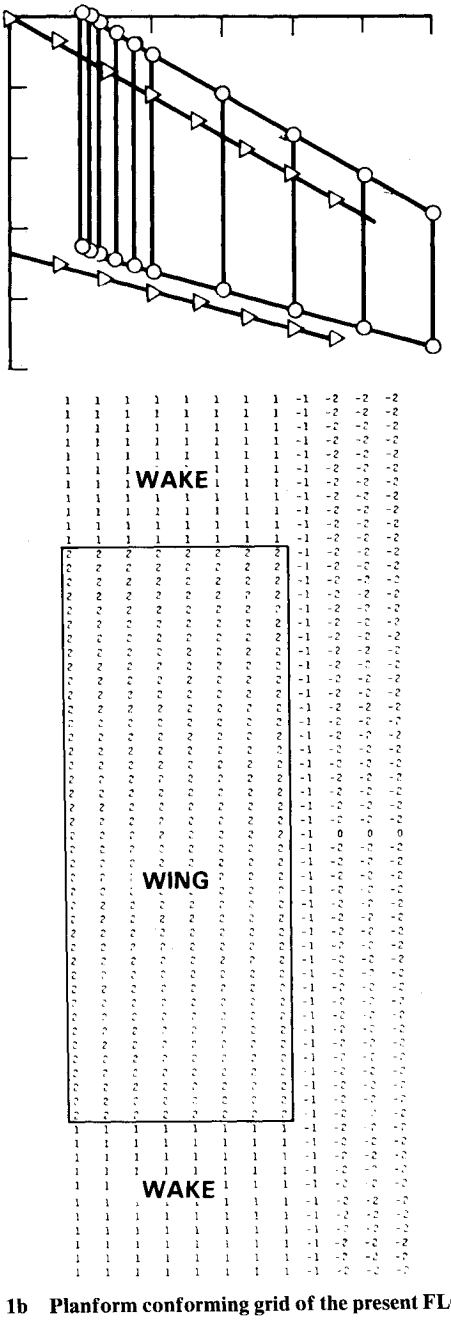

Fig. 1b Planform conforming grid of the present FLO-22.5.

where the reduced potential, G, is defined by $G \equiv \Phi - x\cos\alpha - y\sin\alpha$. The coefficients A through F and the term R are functions of G, partial derivatives of G, and various geometric mapping parameters.[5] The solution of Eq. (2) in the computational domain is subject to the standard Neumann boundary condition on the wing.

Equation (1) transforms a typical section of the wing into a coordinate line in the X-Y plane of the computational space. For rectangular planforms, the trailing edge maps into the coordinate lines $X = \pm C$ where C ℭ a constant determined by the value of F_1. For tapered wings, however, the constant C has a different value for each section. Consequently, the mapped planform does not conform to the actual planform of the wing as illustrated in Fig. 1a. This discrepancy reduces as the total number of grid points increases, i.e., for finer meshes. However, it has an important bearing on the development of a multigrid algorithm which requires transfer of data between coarse and fine meshes. Inaccurate mapping of the trailing edge introduces errors in this transfer for regions around the trailing edge. Another drawback of this transformation is that the number of grid points on an outboard section of a tapered wing is less than that on the root station. This adversely affects the accuracy of flow simulation for wings of moderate to small taper ratio.

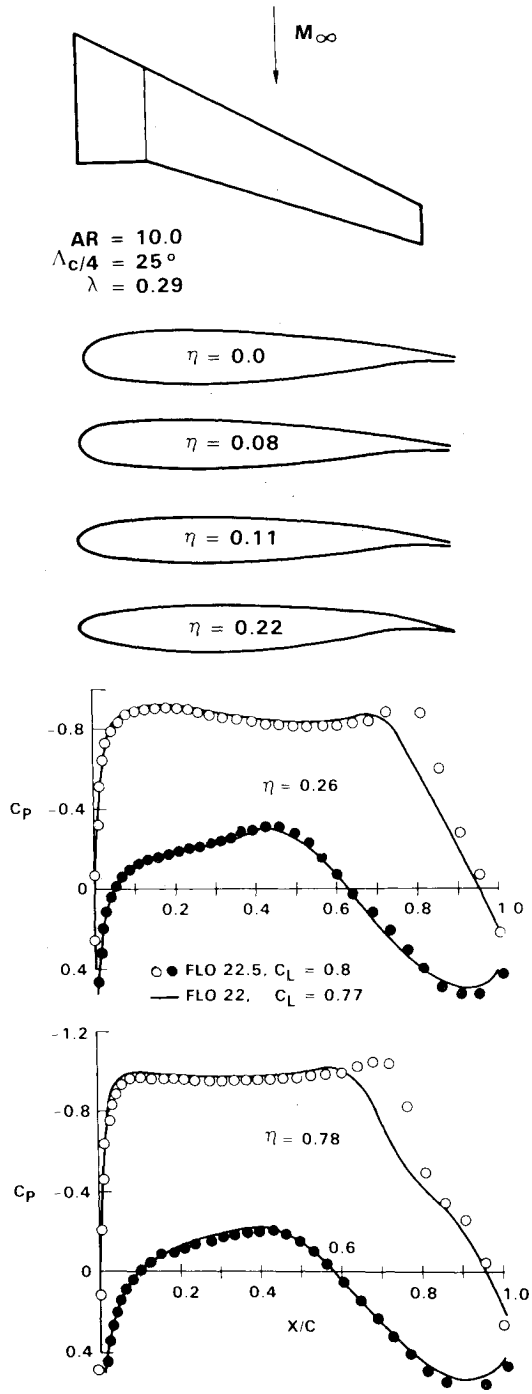

Fig. 2 Improved flow simulation for a typical transport wing at $M = 0.82$, $\alpha = -0.09$ deg.

To alleviate the difficulties described above, the scale factor F_1 in Eq. (1) is redefined to be inversely proportional to the local chord of the wing section. This modification may be interpreted as an additional step requiring the tapered planform to be mapped into a rectangular one before parabolic transformation is invoked. The resulting mesh is planform conforming and the number of grid points is identical for all sections of a wing. This is illustrated in Fig. 1b.

For wings of small taper ratio, the results of the modified code show significant differences when compared to those of the original code. To substantiate this, a typical supercritical wing for transport aircraft is analyzed by using the modified code. The chordwise pressure distributions are compared with the results of the original code in Fig. 2.

Multi-Grid Algorithm

The underlying concept of the multigrid (MGR) technique, as applied to the code under consideration, relies on the fact that the SLOR scheme is efficient in eliminating those components of error whose wavelengths are comparable to the mesh spacing. In other words, the process of liquidating the lower frequency modes is extremely slow on a typical fine mesh. The MGR technique utilizes a sequence of grids of different mesh widths, allowing simultaneous treatment of the whole spectrum of error modes. A variety of algorithms can be developed based on this idea. A complete treatment is beyond the scope of this paper. Interested readers can find very illuminating accounts in Ref. 17 and 18. The outline of a procedure appropriate for the nonlinear equations under consideration is presented here.

Let the discretized form of Eq. (2) on a sequence of grids $D^0, D^1, \ldots, D^K$ of varying mesh spacing be represented by:

$$L^k G^k = F^k, \quad k = 0, 1, \ldots, K \tag{3}$$

since K designates the finest mesh, $F^K = 0$. On coarser meshes, F^k is a forcing function that establishes a link between the truncation errors of a finer and the next coarser mesh. In this crucial aspect, the MGR procedure is different from the sequential grid refining (SGR) currently used in the code. In the SGR approach, an initial calculation is performed on a coarse mesh and the solution is interpolated to a finer grid to obtain a "good" initial solution for the new mesh.

It is easier to think of the MGR procedure as starting on the finest mesh with some initial estimate. When the rate of convergence "stalls", the relaxation process is discontinued on this grid and computations are transferred to the next coarser mesh. While G^k is an approximate solution on D^k, it cannot be expected to be a good approximation on D^{k-1} because of the differences between the discretization errors of the two grids. Therefore, the following equation is relaxed on D^{k-1}:

$$L^{k-1} G^{k-1} = F^{k-1} = R_k^{k-1} F^k + \tau_k^{k-1} \tag{4}$$

where τ_k^{k-1} is the truncation error of the coarse grid relative to the fine grid and this is defined by

$$\tau_k^{k-1} = L^{k-1} R_k^{k-1} G^k - R_k^{k-1} L^k G^k$$

Therefore,

$$F^{k-1} = L^{k-1} R_k^{k-1} G^k + R_k^{k-1} (F^k - L^k G^k) \tag{5}$$

Here R_k^{k-1} is a restriction operator for transferring various quantities from the fine mesh to the next coarse mesh. It should be noted that $(F^k - L^k G^k)$ is the residual left on the fine mesh. The restriction operators for the residual transfer are not necessarily the same as those for transferring the solution.

Once an approximate solution on the coarse grid is computed, the previous solution on the fine mesh is updated. Simply interpolating G^{k-1} will not be correct because the high frequency components of the solution would be lost. These components can be properly retained by adding to the preceding solution G^k the difference between the current solution G^{k-1} on the coarse mesh and its initial estimate, $R_k^{k-1} G^k$. Thus, an improved solution on the fine grid is

$$G^k_{\text{new}} = G^k + P^k_{k-1}(G^{k-1} - R^{k-1}_k G^k) \tag{6}$$

where p^k_{k-1} is an interpolation operator called prolongation operator for transferring quantities from the coarse mesh to the fine mesh. This equation may be written in an alternate form as

$$G^k_{\text{new}} = P^k_{k-1} G^{k-1} + (G^k - P^k_{k-1} R^{k-1}_k G^k) \tag{7}$$

which may be interpreted as follows. Transferring the solution G^k from the fine mesh to the coarse mesh and back to the fine mesh and subtracting the result from G^k provides the contribution of high frequency components. These are added to the interpolated values from the coarse mesh to obtain an improved approximation to the solution on the fine mesh.

To summarize the procedure described above, an approximation to the solution on the fine mesh is first obtained, e.g., by transferring an approximate solution from a coarse mesh. This apprximation on the fine mesh is improved by a "multigrid cycle". This cycle is composed of a few relaxation sweeps followed by a "coarse-grid correction" through Eq. (5). Additional multigrid cycles may be performed for improved accuracy. To solve Eq. (3) on the coarse grid, a combination of relaxation sweeps and corrections from a still coarser grid is employed.

The multigrid approach improves the computational efficiency of the relaxation process by performing most of the work on the coarser meshes and reducing the number of relaxation sweeps on the finest mesh. Relaxation on a coarse mesh efficiently suppresses low frequency components. Because of fewer grid points, relaxation is both more effective and less expensive on the coarse mesh. On the finest mesh, only high frequency error modes need to be eliminated requiring few relaxation sweeps.

A fixed Full Multigrid (FMG)-Full Approximation Scheme (FAS) algorithm[17] based on the concept outlined above has been selected here. For nonlinear problems, such as the present one, FAS is the most appropriate one. The fixed strategy implies that a preassigned set of iterations is used

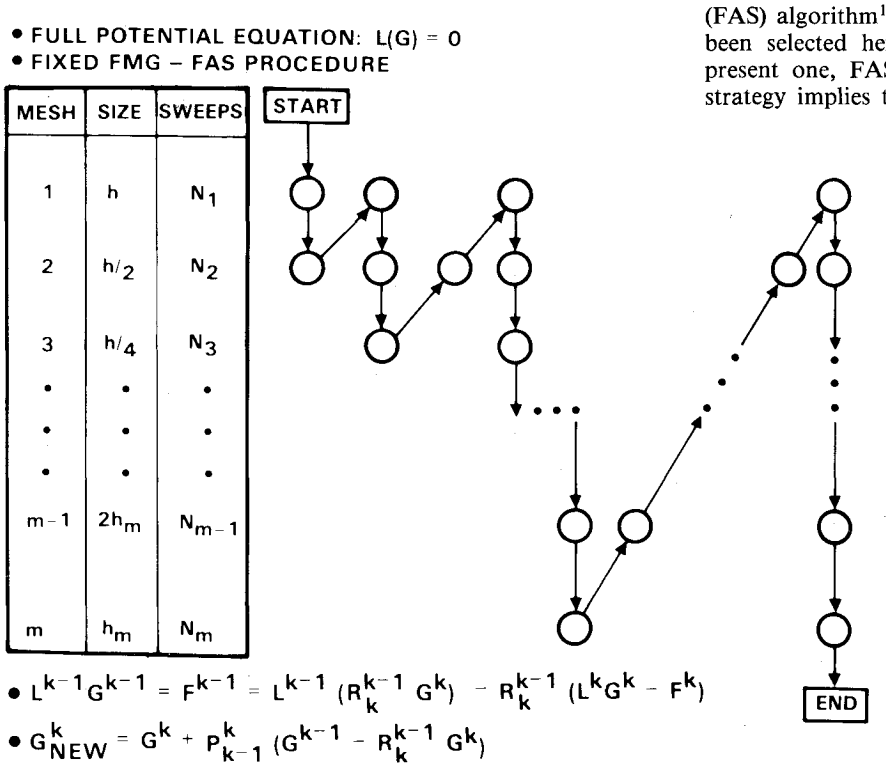

Fig. 3 Fixed full-multigrid, full-approximation scheme.

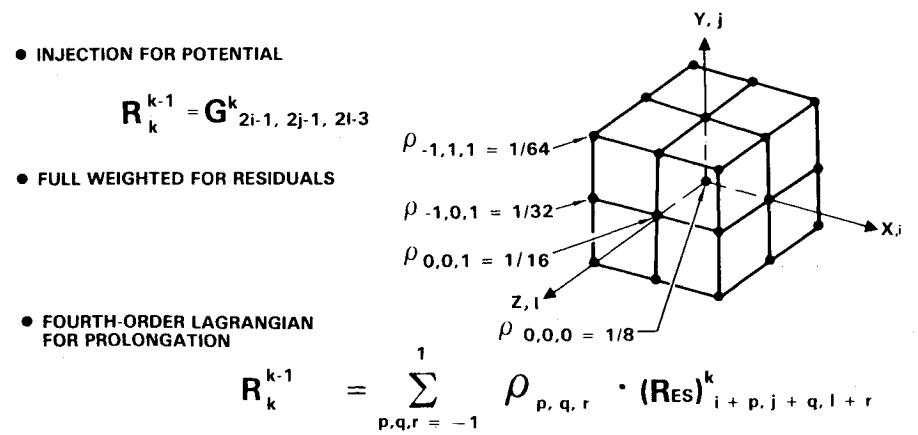

Fig. 4 Interpolation operators.

during each cycle, regardless of the rate of convergence. The use of this strategy was prompted by the fact that it is simpler to program because convergence criteria need not be set up for each of the intermediate grids. A schematic of the procedure is shown in Fig. 3.

In the present version of the multigrid algorithm, each coarse mesh is constructed by eliminating every other grid point of a fine mesh in each direction. On each of these meshes, SLOR sweeps are performed along lines of constant Y. The restriction operator for the transfer of potential, G, is an injection operator, i.e., the value of G from the fine mesh is assigned to the coarse-mesh grid point that is common to both meshes. This is quite convenient, due to the relative structures of the meshes, and also provides the best results. For transfer of residuals, the full weighted scheme of Brandt[18] is utilized. To add the coarse grid corrections, the prolongation operator corresponds to a four-point Lagrangian interpolation. These interpolation operators are schematically shown in Fig. 4.

A guideline in developing the modified solution algorithm was to keep the changes in the original code to a minimum. It decreased the programming effort at the expense of constraining the performance of the resulting code. For instance, large-aspect-ratio cells used in the original code reduce the effectiveness of the relaxation scheme in smoothing the components of error. These cells result from a disproportionate stretching of the grid near the outer boundary of the computational space which corresponds to infinity in the physical space. Another source of difficulty arises from the use of special equations for the vortex sheet and for the grid points on the continuation of the singular line outboard of the wing tip as described in Ref. 5. For swept wings, the nonorthogonality of the mesh also requires a special treatment of the boundary condition on the plane of symmetry. These features introduce errors in transferring various quantities from one mesh to another.

The use of image points across the mapped wing plane to impose the surface boundary condition[5] presents some difficulties in prolongating the correction. The values of potential at the image point can be determined in two ways: 1) use the surface boundary condition after updating the values of potential, or 2) use Eq. (5) for the fine-mesh image points which are located between the boundary points and image points of the coarser mesh. Results depend on the option used, and the choice is not obvious. To remove this uncertainty, explicit use of the image points is eliminated by combining a central difference approximation to the surface boundary condition with the finite difference approximation to Eq. (2) on the boundary. This procedure also has a favorable impact on the rate of convergence of the code in the SGR mode of operation.

As mentioned earlier, the fixed strategy using a specified number of sweeps on each visited grid is used here. One sweep on the finest grid constitutes one work unit (W.U.). For the present three-dimensional problem, the work per sweep on a mesh is given by $\frac{1}{2}^{3(m-n)}$. Here m represents the total number of meshes and n corresponds to the order of the mesh in the sequence of grids, $n=1$ being the coarsest.

Results and Discussion

Analysis Mode

The multigrid version of the FLO-22.5 code has been used to analyze a number of wings. The results for two representative planforms, one rectangular and the other swept, are presented here.

The first wing has a rectangular, constant chord, an untwisted planform, and an NACA 0012 cross section. The aspect ratio of the wing is 8. A primary consideration in the

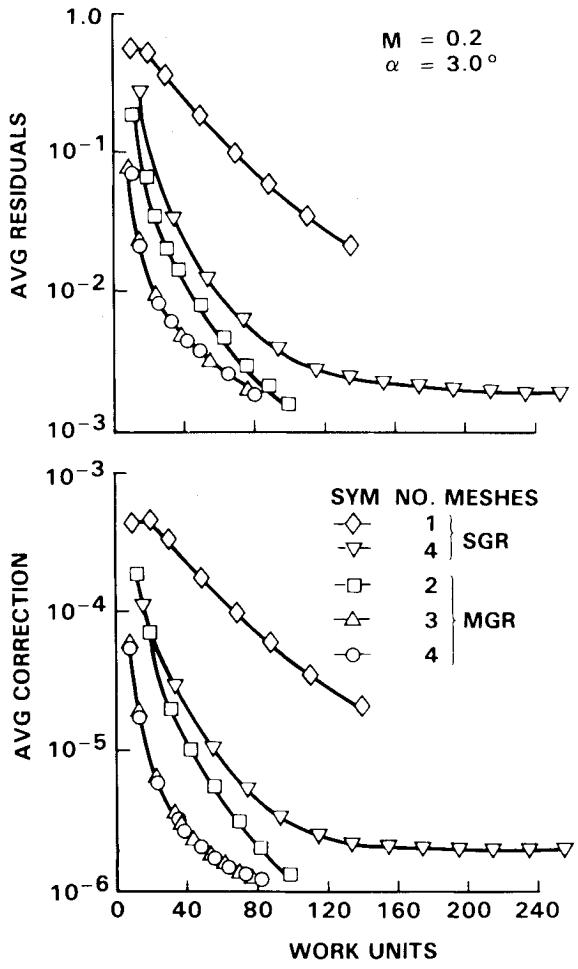

Fig. 5 Subsonic convergence characteristics of FLO-22.5 for a rectangular wing, $AR=8$, NACA 0012 section.

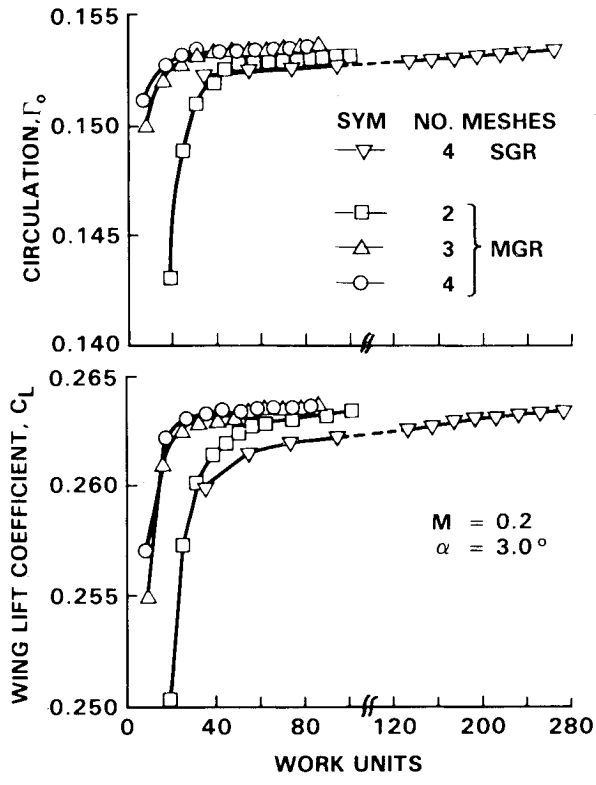

Fig. 6 Subsonic convergence histories of aerodynamic parameters for a rectangular wing, $AR=8$, NACA 0012 section.

selection of this geometry is its simplicity, which eliminates some of the possible sources of errors in the solution. For instance, no special treatment of the boundary condition is needed at the plane of symmetry, as the mesh is orthogonal. For this configuration, two cases are considered: A) $M=0.2$ and $\alpha=3.0$ degrees, and B) $M=0.75$ and $\alpha=1.5$ deg. The governing equations for case A are elliptic, since the flow is entirely subsonic. For case B, transonic nature of the flow requires solution of a mixed elliptic-hyperbolic equation.

In each case, the multigrid algorithm is used with 2, 3, and 4 grids. For the fixed strategy used here, the number of sweeps is to be specified for each grid. A variety of combinations is possible to minimize the total work. Based on numerical experimentation, the following set is employed: 5 sweeps on the finest mesh, and each successive coarse mesh using twice as many sweeps as the preceding fine mesh. The initial value of the potential is set to zero at all of the grid points on the coarsest mesh.

To evaluate the performance of the MGR algorithm, its results are compared with those of the SGR code. In Fig. 5, variations of the averaged absolute residual and averaged absolute correction with cumulative work units are presented. All of these data correspond to the finest mesh ($128\times16\times24$). As expected, the rate of convergence improves with increasing number of meshes in the MGR code. The rates of convergence of the circulation, Γ_0, at the root station and the lift-coefficient, C_L, of the wing, are shown in Fig. 6. Both of these parameters exhibit small changes in the fourth significant digit after three multigrid cycles. Comparable results from the SGR code in its usual mode of operation using four grids require more than 300 W.U. This contrasts with approximately 30 W.U. for the MGR code. For matched C_L of 0.263, the computed surface pressures corresponding to the MGR and SGR versions show identical distributions on the entire wing.

For Case B, transonic flow at 0.75 Mach number, the results are presented in Figs. 7 through 9. The rate of convergence of the averaged absolute residual and averaged absolute corrections exhibit trends similar to those of Case A. An examination of the rates of convergence of Γ_0, number of supersonic points, and wing C_L, as shown in Fig. 8, clearly demonstrates the superiority of the MGR code over the SGR code. The SGR version with 4 grids requires 500 W.U. to asymptotically reach the levels of the various parameters computed by the MGR version in approximately 30 to 40 W.U. while employing the same four grids. In Fig. 9, the computed surface pressure distributions corresponding to the MGR and the SGR versions are compared for identical C_L of 0.1916. No difference is detected between the two sets of distributions.

The second planform considered in this paper is the well-known ONERA M6 wing,[21] with an aspect ratio of 3.8, a taper ratio of 0.56, and a leading-edge sweep of 30 deg. The selection of this wing was dictated by the fact that it has undergone exhaustive computational investigations and correlations with experimental data.

The MGR version of the present code is used to analyze this isolated wing at a freestream Mach number of 0.84 and an angle of attack of 3.06. In Fig. 10, the computed chordwise pressure distributions are compared with the experimental

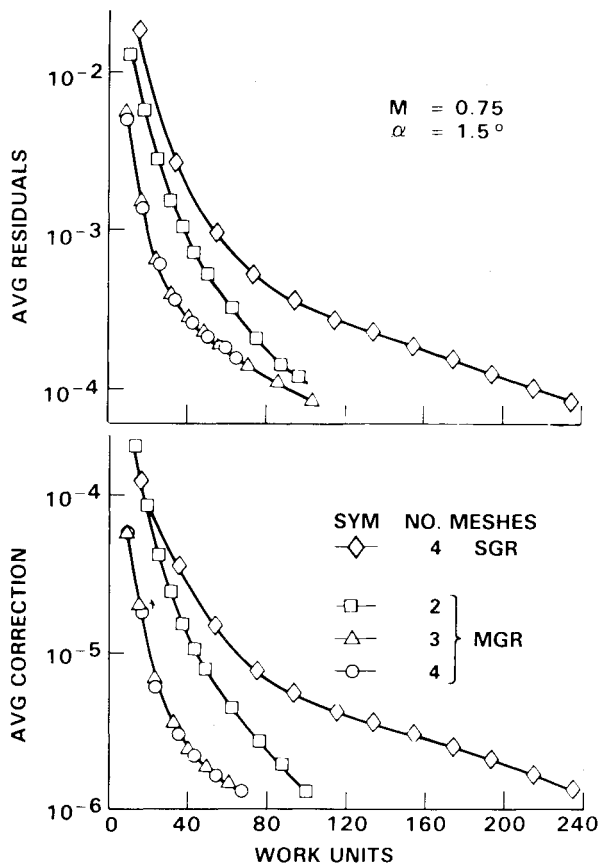

Fig. 7 Transonic convergence characteristics of FLO-22.5 for a rectangular wing, $\mathcal{R}=8$, NACA 0012 section.

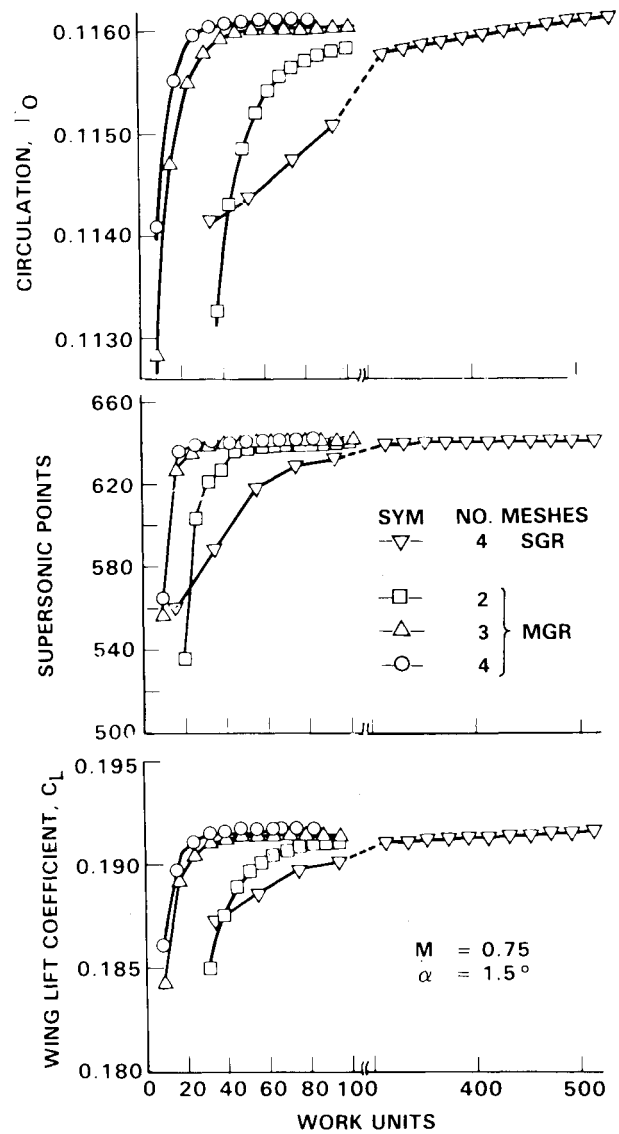

Fig. 8 Transonic convergence histories of aerodynamic parameters for a rectangular wing, $\mathcal{R}=8$, NACA 0012 section.

data[21] at four span stations. Computational results correspond to two different fine meshes. One of these has 96, 16, and 16 intervals in X, Y, and Z directions, respectively, and the other mesh has 192, 16, and 32 intervals. For both meshes, the wing aerodynamic parameters are essentially converged in approximately 30 work units. This contrasts the recommended typical SGR mode of operation requiring more than 100 work units.[5] The results of the refined mesh are in closer agreement with the experimental data than those of the coarser mesh, as one might expect. The results on the refined mesh also agree very well with those in Fig. 8 of Ref. 5 for the original FLO-22 code using a $192\times16\times32$ mesh. The discrepancy between the computational and experimental results may be attributed to the lack of viscous effects and the inherent approximations in the FPE formulation.

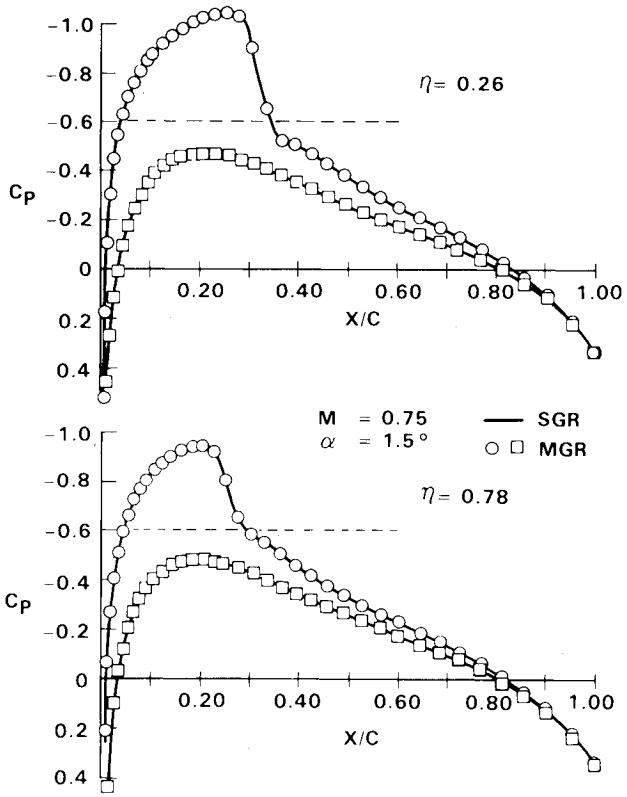

Fig. 9 Comparison of computed typical chordwise pressure distributions using SGR and MGR versions of FLO-22.5 for a rectangular wing, $\mathcal{R}=8$, NACA 0012 section.

It must be pointed out that certain aspects of the present algorithm need further study. In particular, the stalling of the rate of convergence following a few multigrid cycles, as illustrated in Figs. 5 and 7, is of concern. The data indicate that there are regions of the computational domain near the outer boundaries where the residuals and corrections are relatively large, even though the solution appears to be essentially converged on the wing. The latter is evidenced by the values of the aerodynamic parameters shown in Figs. 6 and 8. Other investigators[20,22] have recommended that the solution at all points of the computational domain, including boundary points, be calculated by the same relaxation algorithm. Careful treatment is required if special operators are used. In the basic formulation of the present SLOR scheme, some regions of the boundary are treated differently than the interior points, as discussed in Ref. 5. The contribution of these factors, along with the effect of grid stretching, has to be investigated in more detail. Some benefit could possibly be obtained[22] by sweeping along lines of constant X in addition to the Y-sweep used in the present version.

Design Mode

The present FLO-22.5 code incorporates a wing design procedure based on the formulation proposed by Garabedian and McFadden.[16] Starting from a baseline geometry and flow conditions, the initial surface pressure distribution is computed by the code. The results are examined to select the span stations that need modifications. At these stations, the chordwise extents of the regions to be modified are delineated and a "target" pressure distribution is generated. A modified surface that is compatible with the target values is obtained by numerically integrating a partial differential equation, as described in Refs. 13 and 16.

In a typical design exercise, the MGR version of the present code is used for the initial analysis. The surface modification is carried out on the finest mesh, using an iterative scheme that consists of one surface update followed by one relaxation sweep. The number of iterations depends on the difference between the initial and the target pressure levels. The capabilities of the procedure are illustrated by the results in Fig. 11 for a supercritical wing for a transport aircraft. Sections outboard of the 40% span station are modified to obtain an essentially shock-free flow. This example required approximately 150 work units. The redesigned wing has lower wave drag than the original wing. Reduced likelihood of a shock-induced separation on the modified wing should provide additional aerodynamic benefits.

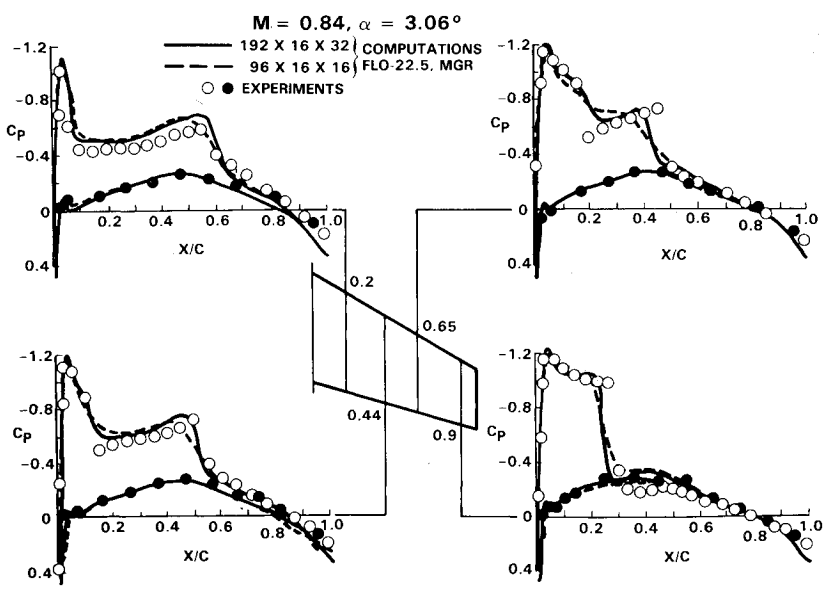

Fig. 10 Comparison of computational and experimental chordwise pressure distributions for ONERA M6 wing.

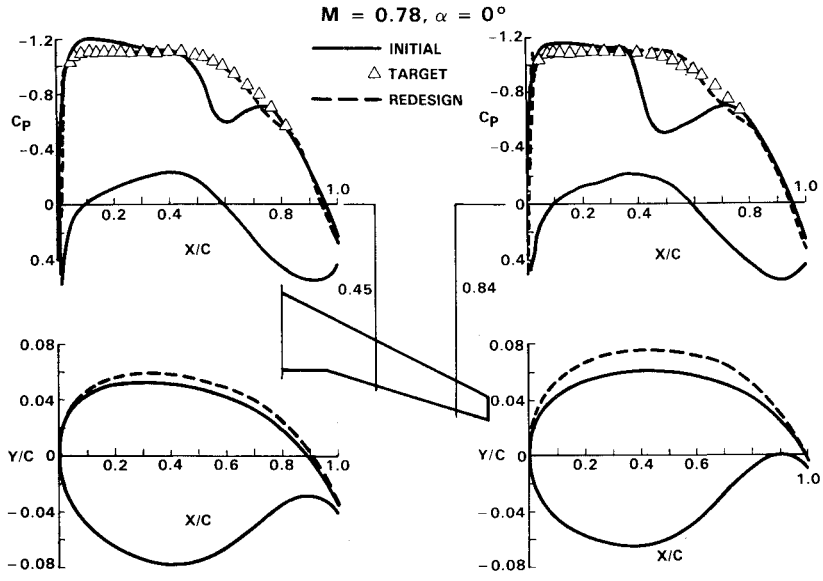

Fig. 11 Example of a supercritical wing redesign using FLO-22.5.

The effectiveness of the design procedure is enhanced by the modifications to the FLO-22 code described in this paper. This results from improved accuracy of flow simulation on the outboard stations and reduced computational work units for the initial analysis phase.

Conclusions

From the results presented in this paper and other data, it may be concluded that incorporation of the multigrid procedure into the solution algorithm considerably improves the computational efficiency of the FLO-22 code. For routine practical applications, the multigrid algorithm reduces the computational time while yielding a better approximation to the converged solution. Additional improvement in the accuracy of flow simulation for wings with small taper ratio is achieved by modifying the geometric transformation relating the physical domain to the computational domain. This gives a planform conforming mesh, thereby eliminating another limitation of the original code. These modifications also have a favorable impact on the design procedures based on the present code.

Acknowledgments

This work is supported by the Lockheed-California Company Independent Research and Development program. The author wishes to thank L. R. Miranda for suggesting the problem and for continued support and encouragement.

References

[1] Bailey, F.R. and Ballhaus, W.F., "Comparisons of Computed and Experimental Pressures for Transonic Flows about Isolated Wings and Wing-Fuselage Configurations," NASA SP-347, 1975, pp. 1213-1231.

[2] Boppe, C.W., "Transonic Flow Field Analysis for Wing-Fuselage Configurations," NASA CR-3243, 1980.

[3] Mehta, U. and Lomax, H., "Reynolds Averaged Navier-Stokes Computations of Transonic Flows-the State-of-the-Art," Progress in Astronautics and Aeronautics, Vol. 81, *Transonic Aerodynamics,* David Nixon, ed., AIAA, New York, 1982, pp. 297-361.

[4] Jameson, A., Schmidt, W., and Turkel, A., "Numerical Solutions of the Euler Equations by Finite Volume Method Using Runge-Kutta Time-Stepping Schemes," AIAA Paper 81-1259, 14th Fluid and Plasma Dynamics Conference, Palo Alto, Calif., June 1981.

[5] Jameson, A. and Caughey, D.A., "Numerical Calculation of the Transonic Flow Past a Swept Wing," New York University ERDA Report COO-3077, 1977.

[6] Chattot, J.J., Coulombeix, C. and da Silva Tome, C., "Calculs d'ecoulements Transoniques Autour d'ailes," La Recherche Aerospatiale, No. 4, 1978, pp. 143-159.

[7] Sankar, N.L., Malone, J., and Tassa, Y., "A Strongly Implicit Procedure for Steady Three-Dimensional Transonic Potential Flows," AIAA Paper 81-0385, 19th Aerospace Sciences Meeting, St. Louis, Mo., Jan. 1981.

[8] Holst, T.L. and Thomas, S.D., "Numerical Solution of Transonic Wing Flow Fields," AIAA Paper 82-0105, 20th Aerospace Sciences Meeting, Orlando, Fla., Jan. 1982.

[9] Caughey, D.A. and Jameson, A., "Progress in Finite-Volume Calculations for Wing-Fuselage Combinations," *AIAA Journal,* Vol. 18, No. 11, Nov. 1980, pp. 1281-1288.

[10] Thomas, S.D. and Holst, T.L., "Numerical Computation of Transonic Flow About Wing-Fuselage Configurations on a Vector Computer," AIAA Paper 83-0499, 21st Aerospace Sciences Meeting, Reno, Nev., Jan. 1983.

[11] Hinson, B.L. and Burdges, K.P., "Evaluation of Three-Dimensional Transonic Codes Using New Correlation-Tailored Test Data," *Journal of Aircraft,* Vol. 18, No. 10, Oct. 1981, pp. 855-861.

[12] Miranda, L.R., "Evaluation of Full Potential Flow Methods for the Design and Analysis of Transport Wings," Progress in Astronautics and Aeronautics, Vol. 81, *Transonic Aerodynamics,* David Nixon, ed., AIAA, New York, 1982, pp. 545-561.

[13] Miranda, L.R., "A Perspective of Computational Aerodynamics from the Viewpoint of Airplane Design Applications," AIAA Paper 82-0018, 20th Aerospace Sciences Meeting, Orlando, Fla., Jan. 1982.

[14] Van der Vooren, J., Van der Kolk, J.Th., and Sloof, J.W., "A System for the Numerical Simulation of Sub- and Transonic Viscous Attached Flow Around Wing-Body Configuration," AIAA Paper 82-0335, AIAA/ASME 3rd Joint Thermophysics, Fluids, Plasma, and Heat Transfer Conference, St. Louis, Mo., June 1982.

[15] Raj, P., Miranda, L.R., and Seebass, A.R., "A Cost-Effective Method for Shock-Free Supercritical Wing Design," *Journal of Aircraft,* Vol. 19, No. 4, April 1982, pp. 283-289.

[16] Garabedian, P. and McFadden, G., "Design of Supercritical Swept Wings," *AIAA Journal,* Vol. 20, No. 3, March 1982, pp. 289-291.

[17] Brandt, A., "Multilevel Adaptive Computations in Fluid Dynamics," *AIAA Journal,* Vol. 18, No. 10, Oct. 1980, pp. 1165-1172.

[18] Brandt, A. and Dinar, N., "Multigrid Solutions to Elliptic Flow Problems," *Numerical Methods for PDE's,* S. Porter, ed., Academic Press, N.Y., 1979, pp. 53-147.

[19] McCarthy, D.R. and Reyhner, T.A., "Multigrid Code for Three-Dimensional Transonic Potential Flow about Inlets," *AIAA Journal,* Vol. 29, No. 1, Jan. 1982, pp. 45-50.

[20] Shmilovich, A. and Caughey, D.A., "Application of the Multi-Grid Method to Calculations of Transonic Potential Flow about Wing-Fuselage Combination," NASA CP-2202, Oct. 1981, pp. 101-130.

[21] "Experimental Data Base for Computer Program Assessment," AGARD-AR-138, May 1979, Appendix B.

[22] Caughey, D.A., "Multigrid Calculation of Three-Dimensional Transonic Potential Flows," AIAA Paper 83-0374, 21st Aerospace Sciences Meeting, Reno, Nev., Jan. 1983.